

Measurement of Spin Wave Instability Magnon Distributions for Subsidiary Absorption in Yttrium Iron Garnet Films by Brillouin Light Scattering

P. Kabos,* G. Wiese, and C. E. Patton

Department of Physics, Colorado State University, Fort Collins, Colorado 80523

(Received 2 September 1993)

The first evidence for a wide distribution in the critical mode wave vectors above the spin wave instability threshold for subsidiary absorption is reported. The Brillouin light scattering (BLS) measurements were done on 4.15 μm thick yttrium iron garnet films with the static field and the 8.47 GHz linearly polarized microwave field in plane. The distribution in the critical mode wave number is broad, with widths of about 0.5×10^4 – $2 \times 10^4 \text{ cm}^{-1}$ and shapes which change with field and power. These results cast doubts on the validity of simple two mode models for the analysis of self-oscillation, chaos, and related effects above threshold.

PACS numbers: 75.30.Ds, 75.50.Gg, 78.35.+c, 78.70.Gq

Spin wave instability at microwave frequencies and powers above the Suhl [1] or parallel pumping [2] threshold leads to a variety of nonlinear effects which are representative of the general class of parametric, self-oscillation, and chaotic phenomena. The main microwave effect is the threshold itself, along with so-called butterfly curves of the instability threshold microwave field amplitude h_{crit} vs the static magnetic field H and explanations based on a wave vector \mathbf{k} -dependent spin wave linewidth [3] and special modifications of the Suhl theory for thin films [4,5]. The specific situation of interest here is subsidiary absorption [3,4] in single crystal yttrium iron garnet (YIG) films. The corresponding butterfly curve has a range of static fields for which h_{crit} vs H is relatively flat, the critical modes have low wave number k values, and the critical mode polar propagation angle θ_k ranges from near 90° to zero. Brillouin light scattering (BLS) has been used to confirm these dependences by direct measurement of the critical mode \mathbf{k} vector at threshold vs static field [6,7].

There are additional effects above threshold, most based on a self-oscillation in the microwave power at kHz or MHz frequencies [8], with changes in these frequencies as a function of power which lead to multistability, period multiplication, intermittency, chaos, and different routes to chaos [9–15]. Different models have been invoked to explain these effects. The simplest model is in terms of *two* spin wave modes sufficiently close in frequency to produce the observed beat in the kHz–MHz range [16–19]. The above threshold problem has also been approached more generally, in terms of renormalized modes [18,19] or the full continuum of spin wave modes [20].

In the above, BLS measurements of \mathbf{k} distributions for the critical modes at threshold provided a key test of the basic instability theory. Measurements for the *above threshold* situation could provide key information for the interpretation and modeling of the self-oscillation, chaos, and related effects for magnetic systems in particular and for nonlinear collective excitations in general. This paper

reports the first Brillouin light scattering measurements of such \mathbf{k} distributions for the critical spin wave modes excited above the spin wave instability threshold. The experiments were done on 4.15 μm thick single crystal (111) YIG films. The static and linearly polarized microwave magnetic fields were both in plane and mutually perpendicular. The BLS spin wave measurements were obtained in a forward scattering configuration by the technique described by Wettling *et al.* [6] and Wilber *et al.* [7,21]. This technique allows determination of the distribution of both the in-plane component of \mathbf{k} and the angle θ_k between this \mathbf{k} component and the static field H . From the work of Wiese, Kabos, and Patton [4], the critical mode wave vector \mathbf{k} at threshold is in plane, so that the measured in-plane component of \mathbf{k} is the wave number k and θ_k is the usual polar spin wave propagation angle. These k and θ_k distributions were measured as a function of the microwave power above the threshold for various values of the static field H in the low k region of the butterfly curve.

The experiments were done by placing the film on an inside wall of a rectangular TE₁₀₂ reflection microwave cavity, modified for optical access. Continuous wave microwave power was applied at the cavity frequency of 8.47 GHz. The power levels were kept low enough to avoid heating effects, while still high enough to examine the nonlinear response above threshold. Calibrations were based on an assumed minimum value of the spin wave instability threshold microwave field amplitude of 0.3 Oe, typical for subsidiary absorption in single crystal YIG films at 9 GHz [6,7,21]. Light of 488 nm wavelength was incident perpendicular to the surface of the film. The forward scattered light was collected by a lens and directed into a Sandercock type high contrast multipass Fabry-Pérot interferometer (FPI) [22]. The wave number k of the observed spin wave excitation is determined by the forward scattering geometry. For first order spin wave instability, the frequency of the excitation is at one-half the microwave pump frequency. A gate pulse arrangement [21] was used to sample the BLS sig-

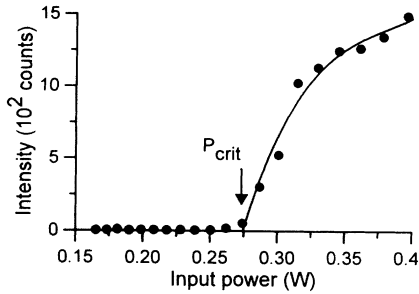


FIG. 1. Representative measurement of the BLS intensity at one-half the pump frequency as a function of the microwave power incident on the cavity for a 4.15 μm thick YIG film in the subsidiary absorption configuration with both the static and linear polarized microwave fields in plane. The static magnetic field was 1290 Oe and the pump frequency was 8.47 GHz. The break point at P_{crit} indicates the spin wave instability threshold.

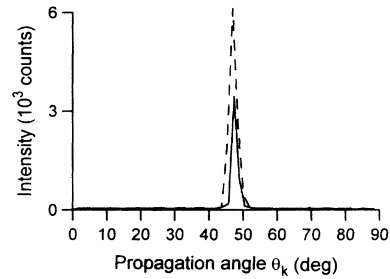


FIG. 2. Representative measurement of the gated BLS intensity at one-half the pump frequency as a function of the in-plane wave propagation angle θ_k . The static magnetic field was 1350 Oe and the pump frequency was 8.47 GHz. The solid line is for a power level 5.9 dB above the spin wave instability threshold but still low enough to preclude self-oscillation in the reflected power from the cavity. The dashed line is for a power level 8.3 dB above threshold, a level for which there is self-oscillation.

nal for this half-frequency point only. Propagation angle θ_k and wave number k selection was accomplished by means of a circular diaphragm with a 200 μm wide slit across the diameter. For θ_k selection, the diaphragm was centered on the collection optics axis and rotated. For k selection, the diaphragm was displaced off axis and then rotated. The accuracy of the angle determinations was about $\pm 2^\circ$ and the resolution in k was about $0.01 \times 10^4 \text{ cm}^{-1}$. The range of accessible k values was $(0-4) \times 10^4 \text{ cm}^{-1}$. Measurements of the critical mode BLS scattering intensity vs microwave power, propagation angle θ_k , or wave number k were obtained by changing either the input microwave attenuator, the centered diaphragm orientation, or the displaced diaphragm orientation while monitoring the gated FPI output signal.

Typical results on BLS intensity vs incident microwave power are shown in Fig. 1. The static magnetic field was 1290 Oe, close to the center of the low threshold, and low k flat part of the subsidiary absorption butterfly curve. The results parallel the usual microwave data on loss vs power for spin wave instability [23]. At low power, the scattering signal is essentially zero because no half-frequency spin waves are excited. At some critical power, noted as P_{crit} in Fig. 1, the scattered signal increases abruptly. The onset point in Fig. 1 corresponds to $h_{\text{crit}} \approx 0.3$ Oe, typical for low linewidth single crystal YIG materials [7].

Figure 2 shows representative data on BLS intensity vs in-plane propagation angle θ_k for an external static field of 1350 Oe, also in the middle region of the butterfly curve. The solid line is for a power 5.9 dB above the instability threshold but still below the threshold for self-oscillations. The dotted line is for a slightly higher power in the self-oscillation region. Both curves indicate a very narrow single peak centered at a critical mode propagation angle $\theta_k^{\text{crit}} \approx 46^\circ$. The peak width is a few degrees and is independent of the power above threshold.

Figures 3(a) and 3(b) show the results of measure-

ments of h_{crit} and θ_k^{crit} vs static field H , respectively, over the low wave number region of the butterfly curve. The light scattering limitation to k values below $4 \times 10^4 \text{ cm}^{-1}$ from the size of the collection lens precluded measurements for static fields below the kink point at $H \approx 1050$ Oe. The data show the basic features of the butterfly curve, with the flat h_{crit} region from the kink point to the butterfly curve minimum at $H \approx 1650$ Oe, and the corre-

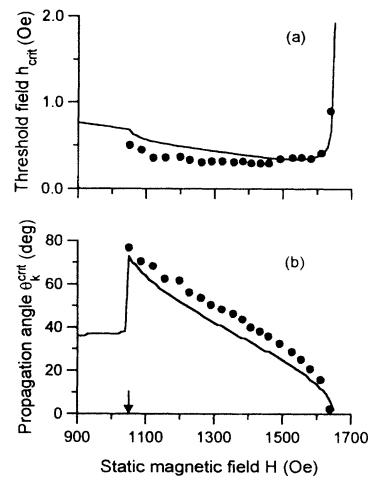


FIG. 3. Summary of results on (a) the spin wave instability threshold microwave field amplitude h_{crit} and (b) the critical mode in-plane propagation angle θ_k^{crit} as a function of the static in-plane magnetic field H over the low wave number minimum threshold region of the subsidiary absorption butterfly curve. The measurements are shown by the solid circles. The minimum h_{crit} point was taken to be at 0.3 Oe. The solid lines show theoretical curves based on the Suhl formalism and parameters from Ref. [7]. The kink point at $H \approx 1050$ Oe is indicated by the arrow on the lower H axis.

sponding variation in the critical mode propagation angle θ_k^{crit} from about 80° down to zero over this region. The solid lines in Figs. 3(a) and 3(b) show calculated values of h_{crit} and θ_k^{crit} vs H based on the procedure of Refs. [3] and [7]. These curves contain an *ad hoc* static field shift of -140 Oe to match the kink point to the data and to accommodate anisotropy effects and differences in the YIG film saturation induction from the literature value of 1750 G.

The sharp θ_k^{crit} distributions made possible a simple and direct measurement of the light scattering intensity as a function of the wave number k . This was done by first displacing the selection diaphragm off the optic axis and then rotating the diaphragm by means of a slow motor drive. Properly calibrated, scans of BLS intensity vs angle yielded profiles of critical mode intensity vs k . Such profiles for different values of the static field H and as a function of power level above the instability threshold at a given H value constitute the central results of this work.

Representative sets of such profiles of scattering intensity vs k for three different field values are shown in Fig. 4. The power levels for the traces are given in dB above threshold. Profile set (a) is for a static field of 1050 Oe and a measured field θ_k^{crit} value of 76° , close to the kink

point on the butterfly curve. Profile set (b) is for a static field of 1290 Oe and a measured field θ_k^{crit} value of 50° , in the middle of the low k part of the butterfly curve. Profile set (c) is for a static field of 1565 Oe and a measured field θ_k^{crit} value of 23° , close to the butterfly curve minimum. All the profiles show that the critical mode k values have broad distributions over the entire low k region of the butterfly curve, and for powers from just above to well above threshold. For profile set (a), the distributions are about $1 \times 10^4 \text{ cm}^{-1}$ in width and show considerable structure. While the width does not change appreciably with increasing power, the structure in the individual profiles changes quite a lot. The numerous small peaks in the profiles for profile set (a) are distinct and reproducible. Most likely, these peaks correspond to various magnetostatic modes which are involved in the nonlinear response [5]. Profile set (b) shows much narrower distributions with widths of about $0.5 \times 10^4 \text{ cm}^{-1}$ as well as quite a different evolution with increasing power compared to the lower field data. Here, one starts out with a single peak centered at about $2.7 \times 10^4 \text{ cm}^{-1}$. As the power increases, this peak drops in intensity, and, at the same time, a second peak at about $2 \times 10^4 \text{ cm}^{-1}$ grows in intensity. At very high powers, a third peak begins to develop at 1.5×10^4 – $1.7 \times 10^4 \text{ cm}^{-1}$. Profile set (c), representative of fields near the butterfly curve minimum, is qualitatively the same as for fields near the kink, except that the distributions are about twice as broad.

It is important to note that the results in Fig. 4 give magnon distributions vs wave number at fixed static field. The work in Ref. [6] for parallel pumping in YIG films concerned parametric magnon distributions vs static field at fixed wave number. The focus in that early result was on the direct determination of the properties of the critical modes associated with first order instability for the specific case of parallel pumping. The focus here is on unexpectedly broad magnon distributions above threshold.

As already mentioned, instability processes above threshold can lead to additional effects such as a spontaneous self-oscillation in the reflected microwave power in the kHz or MHz range, chaos, etc. While these effects are not the focus of this work, one simple experiment was done to explore possible connections between the k distributions obtained above and these higher order nonlinear phenomena. This experiment was to measure θ_k and k distributions of the half-frequency spin waves above threshold but with and without the occurrence of self-oscillations. The onset of self-oscillations was determined by monitoring the reflected microwave signal from the cavity on an oscilloscope. The solid and dashed lines in Fig. 2, already discussed, show the measured θ_k distributions 5.9 dB above the threshold point, with no self-oscillation, and at a higher power 8.3 dB above threshold in the self-oscillation regime. These data show essentially no change in the θ_k distribution with microwave power, with or without self-oscillations. Measurements were also

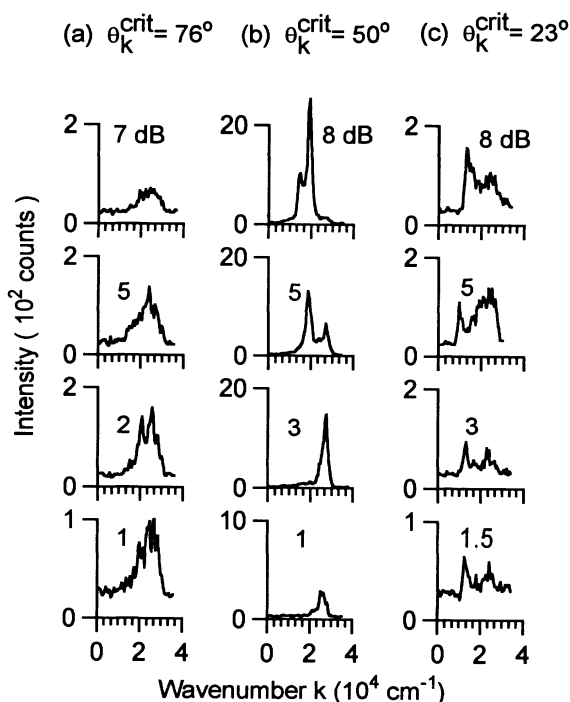


FIG. 4. Experimental profiles of BLS intensity vs in-plane wave number component k for three different values of the static magnetic field H in the low k region of the subsidiary absorption butterfly curve. The microwave pump frequency was 8.47 GHz. Profile set (a) is for $H \approx 1050$ Oe and $\theta_k^{\text{crit}} = 76^\circ$. Profile set (b) is for $H \approx 1290$ Oe and $\theta_k^{\text{crit}} = 50^\circ$. Profile set (c) is for $H \approx 1565$ Oe and $\theta_k^{\text{crit}} = 23^\circ$. The power level for each profile is given in dB above threshold.

made of k distributions just below and just above the self-oscillation threshold. These data also show little change for the distributions without and in the presence of self-oscillations.

In summary, Brillouin light scattering has been used to determine experimentally the distributions in magnon wave vector for the critical spin wave modes excited above threshold in spin wave instability experiments. These distributions are quite broad and indicate that many modes are involved. These results have important implications for the theoretical modeling of nonlinear spin wave processes in magnetic systems and nonlinear processes for collective excitations in general.

Dr. Wiese was supported in part by a fellowship from the Deutsche Forschungsgemeinschaft, Bonn, Germany. The YIG films were provided by Dr. J. D. Adam, Westinghouse Research Laboratories, Pittsburgh, Pennsylvania. The research was supported by the U.S. Office of Naval Research, Grant No. N00014-90-J-4078, the National Science Foundation, Grant No. DMR-89211761, and the U.S. Army Research Office, Grant No. DAAL-03-91-G-0327.

*On leave of absence from the Faculty of Engineering, Slovak Technical University, Bratislava, Slovakia.

- [1] H. Suhl, *J. Phys. Chem. Solids* **1**, 209 (1957).
 [2] E. Schlömann, J. J. Green, and U. Milano, *J. Appl. Phys.* **31**, 386S (1960); F. R. Morgenthaler, *J. Appl. Phys.* **31**, 95S (1960).
 [3] C. E. Patton and W. Jantz, *J. Appl. Phys.* **50**, 7082 (1979).
 [4] G. Wiese, P. Kabos, and C. E. Patton, *J. Appl. Phys.* **74**, 1218 (1993).
 [5] G. Wiese, *Z. Phys. B* **91**, 57 (1993).
 [6] W. Wettling, W. D. Wilber, P. Kabos, and C. E. Patton, *Phys. Rev. Lett.* **51**, 1680 (1983).
 [7] W. D. Wilber, J. G. Booth, C. E. Patton, G. Shrinivasan, and R. W. Cross, *J. Appl. Phys.* **64**, 5477 (1988).
 [8] T. S. Hartwick, E. R. Peressini, and M. T. Weiss, *J. Appl. Phys.* **32**, 223S (1961).
 [9] G. Gibson and C. Jeffries, *Phys. Rev. A* **29**, 811 (1984).
 [10] F. M. de Aguiar and S. M. Rezende, *Phys. Rev. Lett.* **56**, 1070 (1986).
 [11] P. H. Bryant, C. D. Jeffries, and K. Nakamura, *Phys. Rev. A* **38**, 4223 (1988).
 [12] T. L. Carroll, L. M. Pecora, and F. J. Rachford, *Phys. Rev. A* **40**, 377 (1989).
 [13] G. Wiese and H. Benner, *Z. Phys. B* **90**, 119 (1990).
 [14] P. E. Wigen, R. D. McMichael, and C. Jayaprakash, *J. Magn. Magn. Mater.* **84**, 237 (1990).
 [15] F. M. de Aguiar, A. Azevedo, and S. M. Rezende, *J. Appl. Phys.* **73**, 6825 (1993).
 [16] V. E. Zakharov, V. S. L'vov, and S. S. Starobinets, *Sov. Phys. Usp.* **17**, 896 (1975).
 [17] X. Y. Zhang and H. Suhl, *Phys. Rev. B* **38**, 4893 (1988).
 [18] S. M. Rezende and A. Azevedo, *Phys. Rev. B* **45**, 10387 (1992).
 [19] S. M. Rezende, F. M. de Aguiar, and A. Azevedo, *J. Appl. Phys.* **73**, 6805 (1993).
 [20] V. B. Cherepanov and A. N. Slavin, *J. Appl. Phys.* **73**, 6811 (1993).
 [21] W. D. Wilber, W. Wettling, P. Kabos, C. E. Patton, and W. Jantz, *J. Appl. Phys.* **64**, 5479 (1984).
 [22] Interferometer system manufactured by JRS, Ltd. Zwilikerstrasse 8, 8910 Affoltern a. A., Switzerland.
 [23] J. J. Green and T. Kohane, *SCP and Solid State Technology* **7**, 46 (1964).